Jordan Journal of Civil Engineering, Volume **17**, No. **3**, **2023**
DOI: https://doi.org/10.14525/JJCE.v17i3.11

Tension-Stiffening of Reinforced HVFA-SCC Beams

Muhammad Fajrul Falah [1)*], ***Stefanus Adi Kristiawan*** [2)] ***and Halwan Alfisa Saifullah*** [2)]

[1)] Master of Science in Civil Engineering, Faculty of Engineering, Universitas Sebelas Maret, Indonesia.
[2)] Civil Engineering Department, Faculty of Engineering, Universitas Sebelas Maret, Indonesia.
* Corresponding Author. E-Mail: mfajrulfalah@student.uns.ac.id

ABSTRACT

Prediction of cracking behavior and deformation of reinforced concrete is a complex problem, including reinforced concrete that can still bear tensile stress after cracking due to the bond between reinforcement and surrounding concrete, termed the tension-stiffening effect. This research aims to determine the tension-stiffening of reinforced High Volume Fly Ash Self-compacting Concrete (HVFA-SCC) at various tensile reinforcement ratios. In this tension-stiffening analysis, shrinkage and creep effects are taken away. The data used in the analysis was obtained from beams tested with two loading points. The tests were conducted on six reinforced HVFA-SCC beams and six Normal Concrete (NC) beams with dimensions of 150 x 250 x 2000 mm, with tensile reinforcement ratios of 0.61%, 1.10% and 1.55%. The analysis shows that the effect of creep on shrinkage is negligible, so that it can be ignored in the calculation. On the other hand, shrinkage increases the value of the maximum tension-stiffening stress by 1.43% and the ultimate tension-stiffening stress (σts,u) by 72.51% from the initial tension-stiffening values. The greater the tensile reinforcement ratio in concrete, the smaller the effect of tension-stiffening stress.

KEYWORDS: Creep, HVFA-SCC, NC, RC beams, Shrinkage, Tension-stiffening.

INTRODUCTION

As a partial replacement for cement in concrete manufacturing, fly ash can be considered a solution to reduce environmental problems. One of the breakthroughs in concrete technology that utilizes high volumes of fly ash is High Volume Fly Ash Concrete (HVFA). HVFA refers to a type of concrete in which more than 50% of the cement content is replaced by fly ash. On the other hand, a type of concrete has been developed, which is capable of compacting itself, filling mold voids and passing through reinforcement, called Self-compacting Concrete (SCC) (EFNARC, 2002). Combining the concepts of HVFA and SCC is one of the efforts to obtain strong and sustainable concrete (Alghazali and Myers, 2019).

Reinforced-concrete construction can work well in carrying loads if the stress-transfer mechanism between reinforcement and concrete can take place properly as if it had the behavior of a homogeneous material. The stress transfer from concrete to reinforcement is influenced by the adhesion strength between concrete and reinforcement, one of which is influenced by the mechanical interlock between the ribs in threaded reinforcement and concrete (ACI Committee 408, 2003). In addition, the bond strength is also affected by the type of concrete that binds the reinforcement. Thus, the emergence of new types of concrete provides room for more detailed research on adhesive strength and its accompanying structural-performance consequences.

Prediction of cracking behavior and deformation of reinforced concrete beams is a complex problem (Bischoff and Paixao, 2004; Sokolov et al., 2010). It is because reinforced concrete can still bear tensile stress after cracking due to the bond between the reinforcement and the surrounding concrete, which is termed the tension-stiffening effect (Stramandinoli and La Rovere, 2008). In research on moment-curvature relationships, it is stated that tension-stiffening is the difference between the beam response that takes into account the actual stress of the concrete and that at zero

Received on 19/11/2022.
Accepted for Publication on 24/5/2023.

stress (Gilbert, 2013).

Calculating tension-stiffening is influenced by various factors, Sokolov et al. (2010) have investigated the effect of reinforcement ratio in reinforced concrete on tension-stiffening. Tests were carried out on six beam specimens with dimensions of 280 x 300 x 3000 mm with three variations of tensile bar; namely, Ø10, Ø14 and Ø19 mm. From the test results, it can be concluded that the larger the reinforcement diameter (reinforcement ratio), the smaller the tension-stiffening effect.

Tension-stiffening is also affected by the type of concrete. So far, research on tension-stiffening has been carried out on several types of concrete, including normal concrete (Kaklauskas et al., 2015), SCC (Pandurangan and Mohan, 2016), fiber concrete (Álvaro et al., 2016) and geopolymer concrete (Kumar, Indira and Ganesan, 2019). However, tension-stiffening in HVFA-SCC by flexural testing has never been investigated within the reserchers' limits of knowledge.

One of the problems in reinforced-concrete beams is the occurrence of shrinkage and creep with time. They are noticed by the reduction in the volume of concrete. The reduction in volume is due to the reduction in water content as a result of the loss of moisture in the concrete during the hardening process and at a later age (Gilbert, 2013). Shrinkage creates stresses that not only reduce the breaking moment and cause time-dependent cracking, but also cause the tensile stiffness to decrease over time. In addition, tensile forces due to shrinkage are often eccentric in concrete cross-sections, causing additional bending and deflection (Gilbert, 2013). For this reason, the tension-stiffening analysis must consider the effect of shrinkage and creep. Type of concrete has unique shrinkage and creep characteristics, so there is a need to determine the tension-stiffening that must be adjusted to the type of concrete used.

Kaklauskas and Gribniak (2016) tried to eliminate the effects of shrinkage and creep with the inverse method and direct calculation on the moment-curvature and stress-strain diagrams due to tension-stiffening. They used a reinforced-concrete beam specimen having dimensions of 283 x 299 x 3000 mm at an age of 67 days. It was concluded that the proposed methodology (the inverse method and direct calculation on the moment-curvature and stress-strain diagrams due to tension-stiffening) can be used not only to separate the effects of shrinkage and creep on the determination of tension-stiffening, but also to account for their effects on the short-term deformation of cracked reinforced-concrete structural components.

Gilbert (2013) and Castel, Gilbert and Ranzi (2014) modeled time-dependent deflections caused by shrinkage and creep adjusted by the age-adjusted effective modulus method. This method includes the time-varying nature of tension-stiffening due to time-dependent creep and shrinkage. The research specimens were reinforced-concrete beams with dimensions of 300 x 400 x 3500 mm using compressive reinforcement (2 D10) and tensile reinforcement (3 D16) under standard concrete environmental conditions (T-20°C and RH 70%-100%). It was concluded that modeled time-dependent deflections caused by shrinkage and creep adjusted by the age-adjusted effective modulus method is suitable for the calculation of tension-stiffening, which considers the influence of shrinkage and creep.

Previous research (Kristiawan & Nugroho, 2017; Tucker, 2012) indicated that creep and shrinkage of HVFA-SCC are different in magnitude from those of conventional concrete. For this reason, it is interesting to investigate the tension-stiffening of reinforced HFVA-SCC beams compared to normal concrete by separating shrinkage and creep effects. The study was conducted on three beams with tensile reinforcement ratios of 0.61%, 1.10% and 1.55%. Beam testing was conducted by applying two loading points. The centralized load is applied to the beam through a load-distributing beam.

ANALYSIS OF TENSION-STIFFENING

Determining Tension-Stiffening

The determination of tension-stiffening is derived from the analysis of the behavior of reinforced-concrete beams in resisting bending (moment-curvature), as illustrated in Figure 1. When cracking has not occurred, the stress and strain distributions in the beam are essentially linear. In this condition, the moment-curvature relationship in the cross-section is also linear (point O-A) with the same slope as the bending stiffness of the uncracked section, $Ec.I_{uncr.}$ The moment of inertia of the uncracked section (I_{uncr}) is obtained from the equation:

$$I_{uncr} = \left(\frac{b.h^3}{12}\right) \quad (1)$$

where b = beam cross-section width (m) and h = beam height (m).

If the applied load continues to increase, cracking will occur at the lower edge of the cross-section subjected to the cracking moment (M_{cr}). Cracking occurs when the tensile stress at the lower edge reaches the tensile strength of the concrete. At the time of cracking, the tensile force in the concrete at the crack location will be transferred to the steel reinforcement, so that the effective concrete cross-section in resisting the moment is reduced. In this condition, the moment-curvature relationship follows the OAB line, with the effective moment of inertia (I_{ef}) value obtained from the equation (ACI Committee 435, 2003):

$$I_{ef} = \left(\frac{M_{cr}}{M_s}\right)^3 I_{uncr} + \left(1 - \left(\frac{M_{cr}}{M_s}\right)^3\right) I_{cr} \leq I_{uncr} \quad (2)$$

where Ms = maximum moment due to load, M_{cr} = cracking moment $\left(\frac{f_r.I_{uncr}}{y_t}\right)$, fr = concrete cracking modulus ($fr = 0{,}7.\sqrt{f'c}$) and $y_t = h/2$.

As shown in Figure 1, the stiffness $E_c.I_{ef}$ falls between $E_c.I_{uncr}$ and $E_c.I_{cr}$ depending on the magnitude of the applied moment. When $\frac{M_{cr}}{M_s} > 1$, the beam does not crack, so $I_{ef} = I_{uncr}$, but if $\frac{M_{cr}}{M_s} < 1$, the beam cracks with a slope equal to the flexural rigidity of the cracked section, $Ec.I_{cr}$ (Elaghoury, 2019).

The value of the full crack moment of inertia (I_{cr}) is obtained from the equation:

$$I_{cr} = \frac{b.kd^3}{3} + n.A_s(d - kd)^2 + (2n - 1)A'_{s.}(kd - d')^2 \quad (3)$$

with the location of the neutral axis of the transformed cross-section (kd) obtained from the equation:

$$b.kd.\frac{kd}{2} + (2n - 1)(kd - d')A'_s = n.A_s(d - kd) \quad (4)$$

where $n = \frac{E_s}{Ec}$ and A_s = tensile reinforcement area.

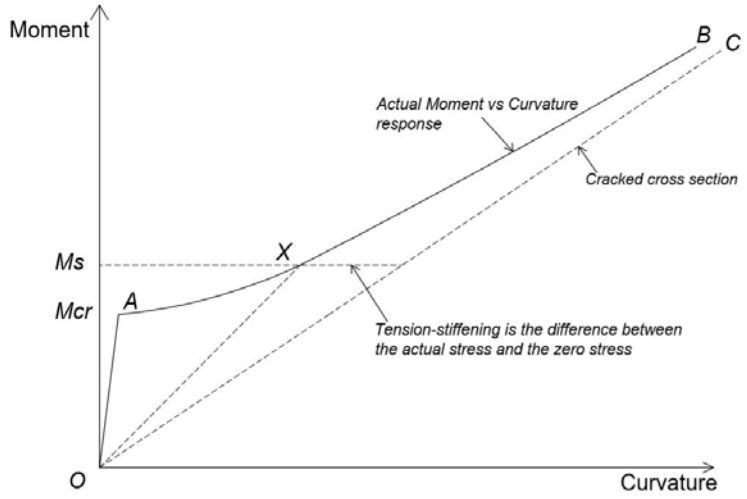

Figure (1): Moment *vs*. curvature (Gilbert, 2013)

The difference between the beam response that takes into account the actual stress of the concrete and that at zero stress is known as tension-stiffening (Gilbert, 2013).

Effect of Shrinkage and Creep on Tension-Stiffening

Shrinkage generally increases over time at a diminishing rate. Shrinkage is relatively faster at the beginning of drying and is proportional to the loss of water during evaporation. The shrinkage strain formula for HFVA-SCC concrete according to Tucker (2012) is highly correlated with the equation (CEB-FIP Model Code, 1990) (See Equation 5). Meanwhile, the shrinkage strain equation for normal concrete, $\varepsilon_{sh,NC}$ according to Eurocode 2 (Gilbert et al., 2017), can be calculated with Equation 6:

$$\varepsilon_{sh,HVFA} = \left[(160 + 10.\alpha_{ds1})\left(9 - \frac{f_{cm}}{f_{cm0}}\right)\right] x10^{-6} x\beta_{RH} x\left[\frac{(t-t_0)/t_1}{350x(h/h_0)^2+(t-t_0)/t_1}\right]^{0.5} \quad (5)$$

$$\varepsilon_{sh,NC} = 0.85\left[(220 + 110.\alpha_{ds1})\, e^{\left(-\alpha_{ds2}\cdot\frac{f_{cm}}{f_{cm0}}\right)}\right] x10^{-6} x\beta_{RH} \quad (6)$$

where:

$$\beta_{RH} = -1.55\left[1 - \left(\frac{RH}{RH_0}\right)^3\right] \quad (7)$$

with f_{cm} = concrete compressive strength, f_{cm0} = 10 MPa, α_{ds1} and α_{ds2}, = cement type-dependent coefficients, RH = relative humidity of the ambient atmosphere (70%), RH_0 = 100%. t = age of concrete, t_0= age of concrete under loading, h = beam height and h_0 = 0.1 m. The formula for finding the value of the coefficient of creep according to (CEB-FIP Model Code, 1990) is:

$$\phi(t, t_0) = \phi_0.\beta_{c(t,t_0)} \quad (8)$$

where ϕ_0 is the notional creep coefficient and $\beta_{c(t,t_0)}$ is a coefficient that shows the development of creep with time after being given loading with the formula:

$$\beta_{c(t,t_0)} = \left[\frac{(t-t_0)}{(\beta_H+t-t_0)}\right]^{0,3} \quad (9)$$

$$\beta_H = 1.55[1 + (0{,}012\, RH)^{18}]h_0 + 250 \quad (10)$$

where t = age of concrete, t_0 = age of concrete under loading, βH = coefficient influenced by relative humidity and concrete size and RH = relative humidity of the ambient atmosphere (%).

After obtaining the shrinkage and creep strain values for each type of concrete and based on the strain compatibility condition, it is necessary to find the equivalent shrinkage strain value that takes into account the creep effect, ε^*_{sh} (Kaklauskas and Gribniak, 2016) through the equation:

$$\varepsilon^*_{sh} = \varepsilon_{sh}\frac{1+np}{1+n_t p} \quad (11)$$

$$p = \frac{A_s}{u}; \quad (12)$$

$$n = \frac{E_s}{E_c}; \quad (13)$$

$$n_t = \frac{E_s}{E_{c,t}}; \quad (14)$$

$$E_{c,t} = \frac{E_c}{1+\phi(t,t_0)} \quad (15)$$

where ε_{sh} = shrinkage strain, u and Ec = area and modulus of elasticity of concrete, As and Es are reinforcement parameters, n and nt = short-term and long-term modular ratios, Ec,t = deformation modulus of concrete obtained by taking into account the effects of creep and $\phi(t, t_0)$ = coefficient of creep.

Steps to Eliminate the Effects of Shrinkage and Creep

Analysis of tension-stiffening by eliminating the effects of shrinkage and creep was carried out following the research by Kaklauskas and Gribniak (2016). The requirement in this analysis is that the amount of tensile reinforcement is equal to the amount of compressive reinforcement, because it is assumed that the tensile concrete stresses of different origins (elastic and tension-stiffening) are represented by the resultant stresses of the concrete with modified deformation characteristics, termed tension-stiffening stresses, act in the area equal to the area of the tensile reinforcement. The principles and procedures of the analysis can be summarized as follows.

Step 1) Using the experimental moment-curvature diagram, the tension-stiffening relationship is derived using the inverse technique. Through this technique, the tension-stiffening stress, σ_{ts} can be calculated with the formula (Kaklauskas and Gribniak, 2016):

$$\sigma_{ts} = \frac{\varphi}{A_s}\left[\frac{E_c\, a^2 b}{2} + (E'_s - E_c)(a - d')A'_s - E_s(d - a)A_s\right] \quad (16)$$

where:

$$a = -\frac{1}{3C_3}\left\{2\bar{C}sin\left[\frac{1}{3}arcsin\left(-\frac{27C_3^2C_0-9C_3C_2C_1+2C_2^3}{2\bar{C}^3}\right)\right] + C_2\right\} \quad (17)$$

with:

$$\bar{C} = \sqrt{C_2^2 - 3C_3C_1} \quad (18)$$

$$C_3 = -\varphi E_C\, b/6 \quad (19)$$

$$C_2 = \varphi E_C\, bd/2 \quad (20)$$

$$C_1 = \varphi(E'_s - E_c)(d - d')A's \quad (21)$$

$$C_0 = -\varphi(E'_s - E_c)(d - d')d'A'_s - M_s \quad (22)$$

where: σ_{ts} = tension-stiffening stress (MPa), φ = experimental curvature (m^{-1}), E_c = modulus of elasticity of concrete (MPa), E_s and E'_s = modulus of elasticity of reinforcing steel (MPa), A_s = area of tensile reinforcement (m^2), A'_s=area of compressive reinforcement (m^2), a = center of gravity of the reinforced-concrete beam cross-section (m), b = beam width (m), d = height from the top fiber to the center of gravity of tensile reinforcement (m) and d' = height from the top fiber to the center of gravity of the compressive reinforcement (m).

The modulus of tension-stiffening, E_{ts} is obtained from the equation:

$$E_{ts} = \sigma_{ts}\,/\varepsilon_c \quad (23)$$

with:

$$\varepsilon_c = \varphi\,(d - a) \quad (24)$$

where E_{ts} = modulus of tension-stiffening (MPa) and ε_c = total strain in concrete.

Step 2) Using the tension-stiffening relationship obtained in step 1, the moment-curvature diagram is calculated using the direct technique.

The shrinkage effect is modeled by using the concept of a fictitious axial force, N_{sh} and a fictitious bending moment, M_{sh} corresponding to the axial stiffness of the net concrete cross-section representing both compressive and tensile concrete (Kaklauskas and Gribniak, 2016).

$$N_{sh} = \varepsilon^*_{sh}[E_c(ab - A'_s) + E_{ts}A_s] \quad (25)$$

$$M_{sh} = N_{sh}(a_c - a) \quad (26)$$

where ε^*_{sh} is the shrinkage strain that accounts for the effect of cracking, E_{ts} = modulus of tension-stiffening (MPa), A_s = area of tensile reinforcement (m^2), A'_s = area of compressive reinforcement (m^2) and "a_c" and "a" are the distances from the top fiber of the cross-section to the center of the net concrete cross-section and the cross-sectional center of gravity of the reinforced concrete beam, with the formulae:

$$a_c = \frac{E_c\left(a^2 b/_2 - d'A'_s\right) + E_{ts}dA_s}{E_c(ab - A'_s) + E_{ts}A_s} \quad (27)$$

$$a = \sqrt{\frac{C_1^2 - 4C_2C_0 - C_1}{2C_2}} \quad (28)$$

with coefficients:

$$C_2 = E_c\, b/_2 \quad (29)$$

$$C_1 = (E'_s - E_c)A'_s + (E_s + E_{ts})A_s \quad (30)$$

$$C_0 = -(E'_s - E_c)\, d'A_s - (E_s + E_{ts})dA_s \quad (31)$$

where E_s and E'_s = modulus of elasticity of reinforcing steel (MPa), E_{ts} = modulus of tension-stiffening (MPa), b = beam width (m), A_s = area of tensile reinforcement (m^2) and A'_s = area of compressive reinforcement (m^2),

Curvature-free shrinkage, φ_{sh} can be calculated as follows:

$$\varphi_{sh} = \frac{M_s + M_{sh}}{Ec.I_{ef}} \quad (32)$$

where M_s = maximum moment on a beam with the two loading points (KN-m), M_{sh} = fictitious bending moment (KN-m) (see Eq.26), E_c = modulus of elasticity of concrete (MPa) and I_{ef} = effective moment of inertia (see Eq.2).

Step 3) Tension-stiffening relationship free of shrinkage, calculated by inverse technique (as step 1) using moment-curvature diagram free of shrinkage (Eq. 16).

EXPERIMENTAL INVESTIGATION

Materials and Mixing Proportions

The coarse aggregate used was crushed stone with a maximum size of 20 mm and the fine aggregate included grading zone 2. The characteristics of coarse and fine aggregates are given in Table 1. Fly ash used in this research is type C fly ash from PLTU Tanjung Jati

Jepara, Central Java, Indonesia. Fly ash contains SiO_2 at 43.82%, Al_2O_3 at 15.58% and FeO at 12.13%; so, the total percentage of the three constituents is 71.53%. CaO content is 8%, while moisture content and loss on ignition are in small amounts.

To obtain self-compacting concrete, a superplasticizer must be added ((Alghazali and Myers, 2019). The superplasticizer used is Consol P 292 AS produced by PT Kimia Beton. Indonesia. To determine the composition of the concrete mixture, a trial mix was carried out with several tests to obtain a compressive strength of 30 MPa. At the time of the trial mix, testing was also carried out to ensure that the concrete satisfies the requirements of SCC. The composition of the concrete mixture obtained from the trial mix is given in Table 2.

Table 1. Aggregate test results

Material	Testing Type				
	Specific gravity (kg/m^3)	**Volume weight (kg/m^3)**	**Infiltration (%)**	**Mud content (%)**	**Fineness modulus**
Coarse aggregate	2.65	1417	2.22	0.78	7.63
Fine aggregate	2.53	1541	3.54	3.4	2.96

Table 2. Mix proportions

Code	Cement (kg/m^3)	Fly Ash (kg/m^3)	Coarse Aggregate (kg/m^3)	Fine Aggregate (kg/m^3)	Water (Lt/m^3)	Superplasticizer (Lt/m^3)
HVFA-SCC	275	275	876	635	176	5.5
NC	450	-	940	870	180	5.0

Table 3. Fresh concrete test results

Testing	Target	Results	Units	Remarks
Slump Flow	650 - 800	670	mm	satisfied
T50	2 - 5	4.65	sec	satisfied
L-box	0.8 – 1.0	0.86	mm/mm	satisfied
V-funnel	6 - 12	9.10	sec	satisfied

To ensure that the concrete mixture meets the SCC requirements, testing of fresh concrete was carried out. The tests carried out were slump test, L-box test and V-funnel test according to the standard (EFNARC, 2002). The concrete mixture must be ensured to meet the requirements of flowability, filling ability and segregation resistance to meet the requirements of self-compacting concrete characteristics. The results of fresh-concrete testing are presented in Table 3.

To determine the quality of concrete, the compressive strength of concrete was tested. The test specimens were cylinders with a diameter of 150 mm and a height of 300 mm according to (ASTM C39, 2005). Tests were carried out at the age of 28 days under a compression test equipment with a capacity of 2000 kN. The results of the concrete-cylinder compressive test are given in Table 4. Meanwhile, reinforcements were tested under a uniaxial testing machine and the results are given in Table 4 as well.

Table 4. Beam specimens

Specimens	Dimensions			Tensile Reinforcement	Concrete Strength, MPa	Steel Yield Stress, MPa	Reinforcement Ratio; μ, %
	Width; b, mm	Height; h, mm	Effective Depth; d, mm				
HVFA-SCC - 12	150	250	231	2 D12	33.12	405	0.61
HVFA-SCC - 16			233	2 D16		415	1.10
HVFA-SCC - 19			234	2 D19		390	1.55
NC - 12			231	2 D12	29.54	405	0.61
NC - 16			233	2 D16		415	1.10
NC - 19			234	2 D19		390	1.55

Beam Test Specimens

The beam specimens were 150 mm wide, 250 mm high and 2000 mm long. Tensile reinforcement was varied using threaded reinforcement with diameters of 12, 16 and 19 mm. Compressive plain reinforcement was used and stirrups were of 8-mm diameter. The thickness of the bottom cover to steel centroid (c_b) was 25 mm, the side cover (c_o) was 25 mm and the value of half the reinforcement net distance (c_s) varied according to the size of the main reinforcement. In all test specimens, stirrups were installed on one-third of the span of the left and right edges with reinforcing bars of 8-mm diameter spaced @70 mm. The installation of the stirrups aimed to prevent shear failure during beam testing.

There were two types of beam test specimens; namely, HVFA-SCC beams and normal-concrete (NC) beams. For each type of specimens, two test beams were made, so that there were a total of twelve beams to be tested. The sketch of the beams can be seen in Figure 2.

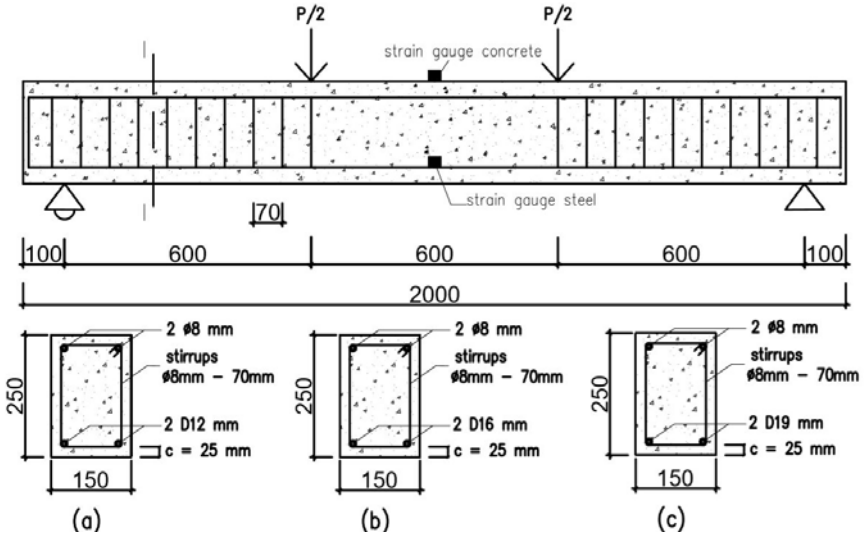

Figure (2): Sketch of the test beam: (a) Diameter of 12 mm, (b) Diameter of 16 mm and (c) Diameter of 19 mm

Testing Set-up

Beam testing was conducted at the Structure Laboratory of Sebelas Maret University, Indonesia. The beam testing set-up can be seen in Figure 3. Beam testing was conducted by applying two loading points. The centralized load is applied to the beam through a load-distributing beam. The distance between the two load points was 600 mm. The distance between the

centralized load and the nearest support was 600 mm (see Figure 2). The beam was supported using a steel pedestal at 100 mm from the end of the beam. The load was measured with a load cell located at the center of the load-distributing beam (Jalil and Sultan, 2021). At the end of the connection, a strain gauge was installed and connected to a strain indicator. The reading of the strain indicator will determine the strain value of the reinforcing steel. Beam deflection at mid-span was measured with two LVDTs mounted on both sides of the beam. Load, strain and displacement readings were recorded on a data logger. Cracks were marked on the beam surface at every 5 kN loading interval.

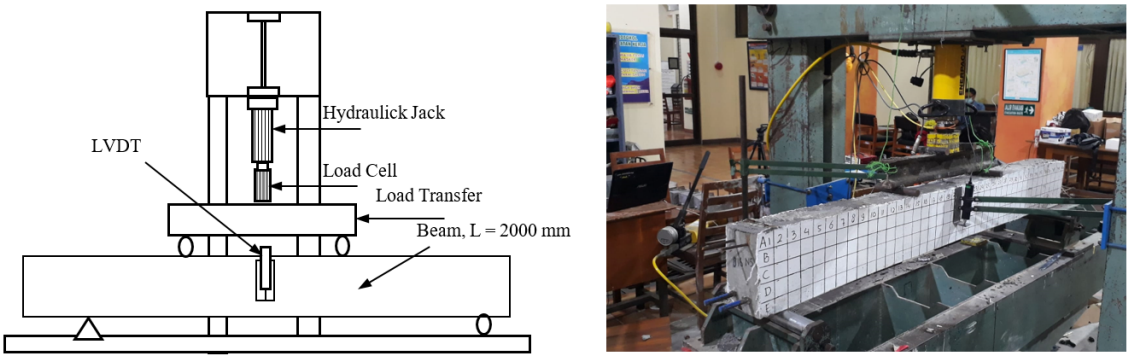

(a) (b)

Figure (3): Beam testing set-up: (a) Testing scheme and (b) Photo of beam testing

DISCUSSION OF RESULTS

Moment *vs.* Curvature

Reinforced-concrete beams are supported by simple pedestals (roller joints) and above the beam work, a centralized load *P* will rise moment.

The experimental mean curvature was determined from readings of the strain gauges mounted on the concrete compression zone and of strain gauges installed at the midspan on the tensile (longitudinal) reinforcements (see Fig. 2).

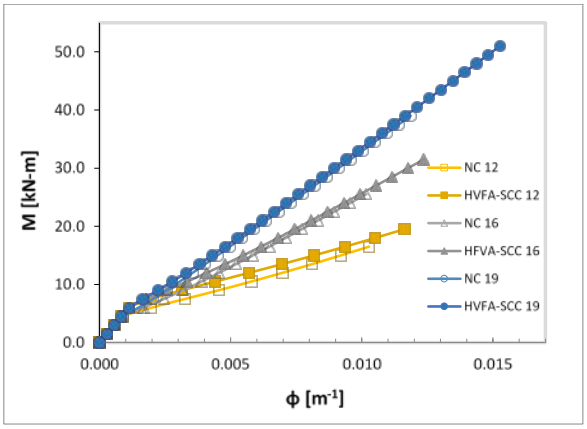

Figure (4): Moment *vs.* curvature curves before removing shrinkage and creep effects

The calculation results of the moment *vs.* curvature curves are presented in Figure 4. The moment-curvature relationship graph in Figure 4 shows the increase in stiffness and the ability of the beam to deform after cracking. From the beginning of loading until the occurrence of the first crack in the beam (in the moment range of 6 to 6.2 kN-m), the curve forms a linear relationship between moment and curvature. Before cracking, the beam can maintain a relatively high stiffness. After reaching the first crack, a moment-curvature curve relationship can be observed where an increase in load will cause a higher curvature value than the preceding load.

Shrinkage, Strain and Creep

The ultimate creep-coefficient value of normal concrete was 2.35, for concrete with fly-ash composition greater than 30% and for environmental conditions different from those specified as standard conditions, a multiplying factor is needed to modify the creep-coefficient value obtained from Eq. 8. Based on Kristiawan & Nugroho (2017), the ultimate-creep value of HVFA-SCC concrete is 3.28. Then, the 50% HVFA-SCC creep coefficient calculated with Eq. 8 needs to be multiplied by the ratio of 1.39 (equals 3.28/2.35). Values of shrinkage strains that take into account the effects of creep, ε_{sh}^{*} calculated using Eqs. 11-15 are given in the

following example and the complete results are presented in Table 5.

Table 5 shows that the shrinkage strain value and the equivalent shrinkage strain have no difference. This indicates that the influence of creep is very small; so, in the procedure to calculate equvalent shrinkage strain ε^*_{sh}, the effect of creep can be ignored.

Table 5. Shrinkage strain, ε_{sh} and equivalent shrinkage strain, ε^*_{sh}

Specimens	ϕ_0	$\beta_{c(t,t_0)}$	$\phi(t,t_0)$	ε_{sh}	ε^*_{sh}
HVFA-SCC - 12	4.363	0.502	2.875	-0.000130	-0.000130
HVFA-SCC - 16	4.363	0.502	2.875	-0.000130	-0.000130
HVFA-SCC - 19	4.363	0.502	2.875	-0.000130	-0.000130
NC - 12	4.120	0.502	2.191	-0.000158	-0.000158
NC - 16	4.120	0.502	2.191	-0.000158	-0.000158
NC - 19	4.120	0.502	2.191	-0.000158	-0.000158

Steps to Eliminate the Effects of Shrinkage and Creep

Step 1

The experimental tension-stiffening stress, σ_{ts} is obtained from Eqs. 16-22. An example of such calculation is given in the subsequent paragraph. The complete results of the calculation are shown in Figure 5, Both for HVFA-SCC and normal concrete (NC), the tension-stiffening stress *vs.* strain curve is shaped like a parabola, where the initial slope of the curve indicates an increase in the strength of the concrete until reaching the peak value. In this phase, the value of tension-stiffening stress σ_{ts} of HVFA-SCC is better than that of normal concrete (NC). For example, the maximum tension-stiffening stress value of HVFA-SCC 12 is 123.5 MPa, while the maximum tension-stiffening stress value of NC 12 is 117.75 MPa (see Table 7). This means that HVFA-SCC concrete is stronger in resisting stress during loading. After attaining the maximum stress, the strain that occurs will increase and indicate a decrease in the strength of the concrete. The decrease of the slope of the tension-stiffening stress (σ_{ts}) *vs.* strain (ε_c) curve is due to cracks that occur in the concrete during loading, which then propagate.

Step 2

After analyzing the experimental moment-curvature as shown in Figure 5, the calculation of moment-curvature by eliminating the shrinkage effect needs to be carried out by Eqs. 25-32. When the effect of shrinkage is eliminated, the moment-curvature curve as presented in Figure 6 is obtained. The details of the reduction in value of curvature are given in Table 6.

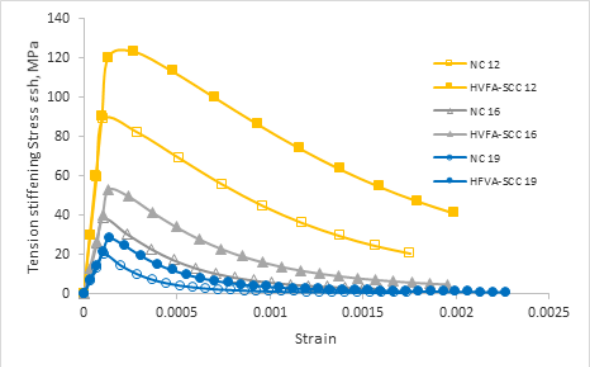

Figure (5): Tension-stiffening stress *vs.* strain before removing shrinkage and creep effects

Table 6 and Figure 6 show that the smaller the tensile reinforcement ratio, the greater the reduction in curvature value due to the shrinkage effect. The curvature-reduction value in HVFA-SCC concrete is smaller than in normal concrete (NC). Overall, the average curvature reduction was -3.76%.

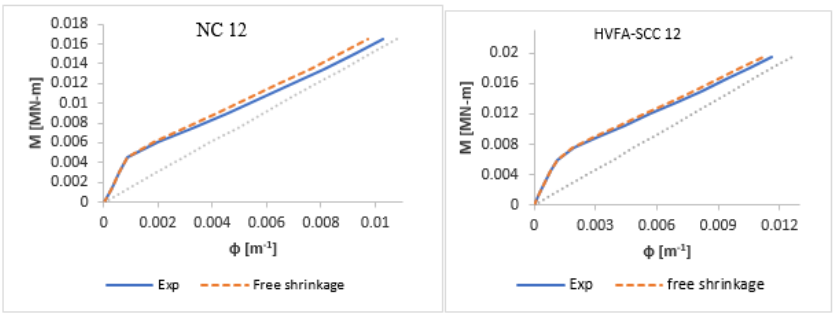

(a) Diameter = 12 mm

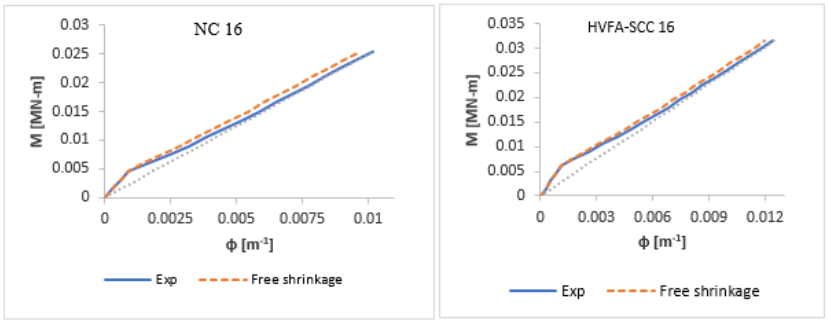

(a) Diameter = 16 mm

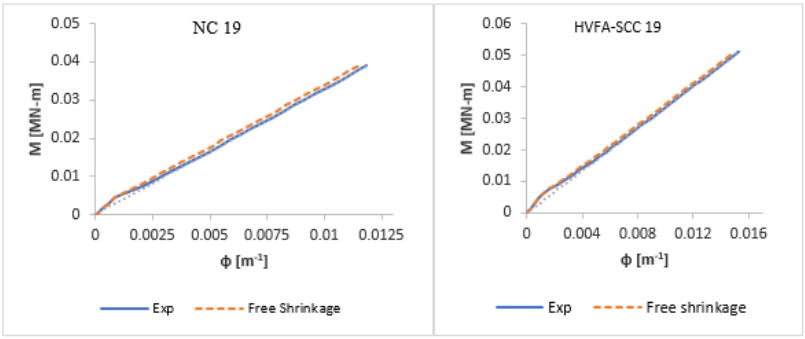

(c) Diameter = 19 mm

Figure (6): Moment *vs.* curvature without shrinkage and creep effects: (a) Diameter = 12 mm, (b) Diameter = 16 mm and (c) Diameter = 19 mm

Table 6. Maximum curvature

Specimens	p (%)	φ_{max} (m^{-1})		% Reduction
		Exp	Free shrinkage	
HVFA-SCC - 12	0.611	0.0116	0.0112	-3.87
HVFA-SCC - 16	1.097	0.0124	0.0120	-3.27
HVFA-SCC - 19	1.554	0.0153	0.0150	-2.04
NC - 12	0.611	0.0097	0.0097	-5.61
NC - 16	1.097	0.0101	0.0097	-4.76
NC - 19	1.554	0.0118	0.0115	-3.03
			AVE	-3.76

Step 3

The shrinkage elimination concept assumes that the tension-stiffening stress (σ_{ts}) is concentrated in the same area where the tensile reinforcement occurs. When performing direct analysis, the total strain value (ε_{tot}) in the tensile reinforcement is determined from the sum of the free shrinkage strain (ε_{sh}) with the stress-induced strain (ε_c) (see Eq. 24); so, it can be written as ($\varepsilon_{tot}=\varepsilon_{sh}+\varepsilon_c$). However, when performing the inverse analysis, the value of the free shrinkage strain (ε_{sh}) is assumed to be = 0; so, the value of $\varepsilon_{tot}=\varepsilon_c$.

As for eliminating the effects of shrinkage and creep on the tension-stiffening stress, it can be calculated using Eq. 16-22 (see the following example) by using the curvature value obtained from Eq. 32 with the results shown in Figure 7. The reduction of tension-stiffening stress *vs.* strain diagram due to the effects of shrinkage and creep is summarized in Table 7.

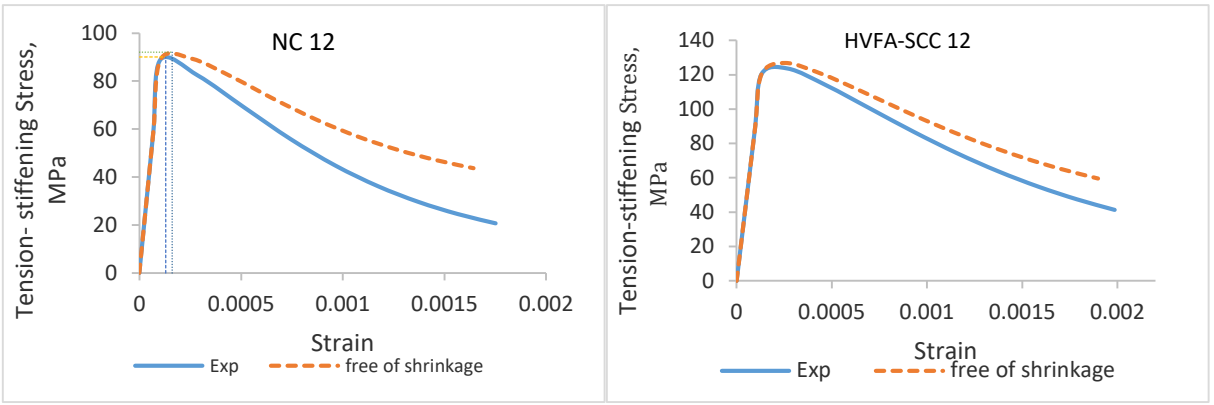

(a) Diameter = 12 mm

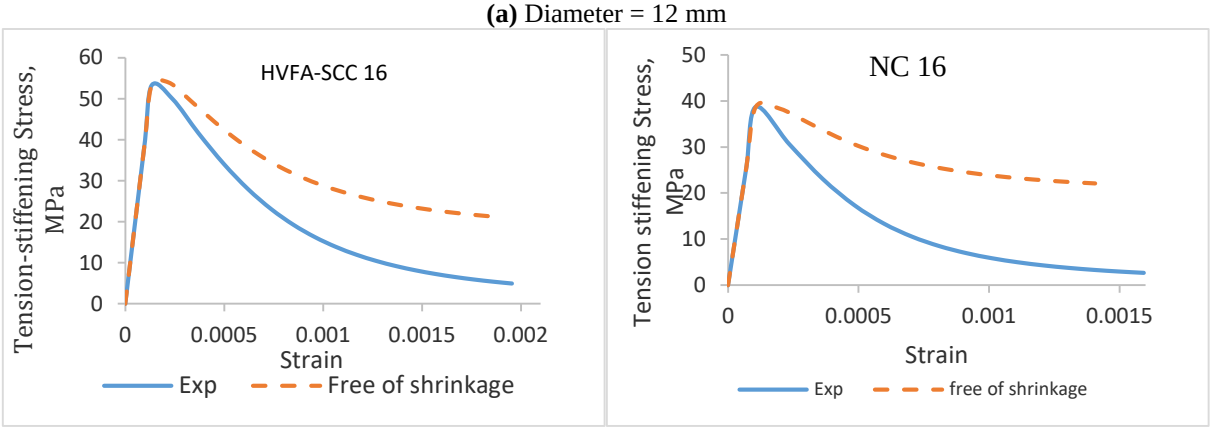

(b) Diameter = 16 mm

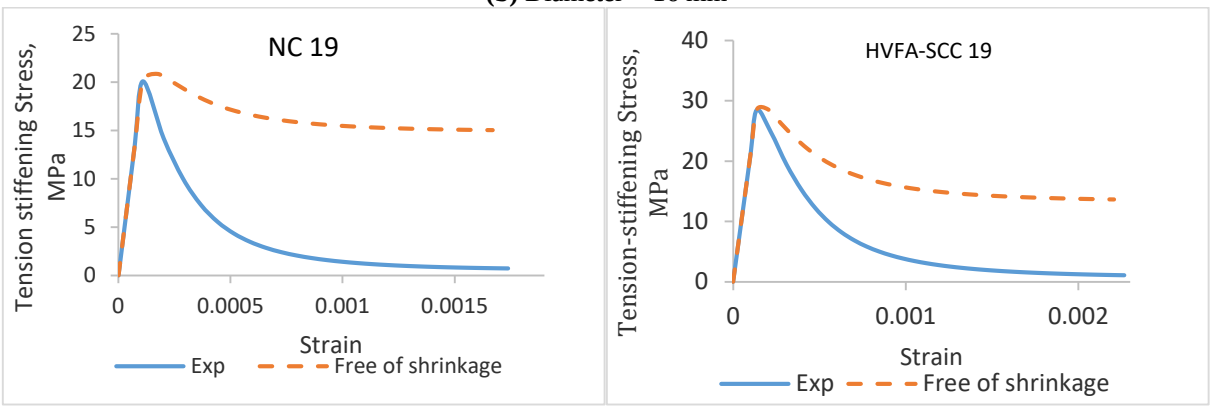

(c) Diameter = 19 mm

Figure (7): Tension-stiffening stress *vs.* strain after removing shrinkage and creep effects: (a) Diameter = 12 mm, (b) Diameter = 16 mm and (c) Diameter = 19 mm

In Figure 7, the graphical relationship of tension-stiffening stress (σ_{ts}) *vs.* strain (ε_c) in HVFA-SCC and normal-concrete (NC) specimens after the elimination of the effects of shrinkage and cracking. The initial slope of the curve indicates the strength gain in the concrete until reaching the maximum stress. In this phase, the curves show the similarity between the experimental and the free-of-shrinkage curves, suggesting that shrinkage has not yet affected the concrete. Subsequently, the strain that occurs after the maximum stress will increase and indicate a decrease in the strength of the concrete. In this phase, differences in shape begin to emerge as shrinkage begins to affect the concrete. As seen in Table 7, the value of $\sigma_{ts\ \max}$ due to shrinkage increases, although not significantly. The slope of the decrease in the tension-stiffening stress (σ_{ts}) *vs.* strain (ε_c) curve is due to cracks that occur in the concrete during loading which then propagate. The maximum strain will decrease as the strength of the concrete increases. In this phase, shrinkage has a significant effect.

Table 7. Effect of shrinkage on tension-stiffening stress *vs.* strain diagram

Specimens	Reinforcement ratios (%)	Tension-Stiffening Stress Maximum, $\sigma_{ts\ \max}$ (MPa)		Tension-Stiffening Ultimate, $\sigma_{ts,u}$ (MPa)		%Reduction of Tension-Stiffening Stress Maximum, $\sigma_{ts\ \max}$	%Reduction of Tension-Stiffening Ultimate, $\sigma_{ts,u}$
		Exp.	Free of shrinkage	Exp.	Free of shrinkage		
HVFA-SCC-12	0.611	123.50	123.50	41.30	59.61	0.00	30.72
HVFA-SCC-16	1.097	53.27	53.90	4.95	21.19	1.18	76.65
HVFA-SCC-19	1.554	28.46	28.57	1.08	13.63	0.38	92.10
NC - 12	0.611	89.01	89.36	20.68	43.67	0.39	52.65
NC - 16	1.097	52.30	53.90	2.69	21.85	2.98	87.70
NC - 19	1.554	20.08	20.85	0.72	15.02	3.66	95.23
					AVE	1.43	72.51

The results of calculating the amount of shrinkage and creep reduction on the tension-stiffening *vs.* stress are given in Table. 7. Table 7 shows that shrinkage is quite influential in concrete calculations, because it reduces the maximum tension-stiffening stress (σtsmax) by at least 1.43% and the ultimate tension-stiffening stress (σts,u) by 72.51%. For this reason, the calculation of tension-stiffening by eliminating shrinkage and creep is necessary to obtain more detailed and accurate calculation results. In Table 7 and Figure 7, it can be seen that the maximum tension-stiffening stress, $\sigma_{ts\ \max}$ is greatest at a reinforcement ratio of 0.611% which is 123.50 MPa and the smallest maximum tension-stiffening stress, $\sigma_{ts,\max}$ is at a reinforcement ratio of 1.554% which is 28.57 MPa. The value of maximum tension-stiffening stress, $\sigma_{ts\ \max}$ of HVFA-SCC concrete is greater than that of NC concrete. This means that the greater the reinforcement ratio in concrete, the smaller the effect of tension-stiffening stress (σ_{ts}). This is in line with Sokolov et al. (2010) and Kaklauskas et al. (2011) who stated that the effect of tension-stiffening will decrease as the reinforcement ratio increases.

SUMMARY AND CONCLUSIONS

Values of shrinkage strains that take into account the effects of creep, ε^*_{sh} show that shrinkage strain value and equivalent shrinkage strain have no difference. This indicates that the influence of creep is negligible; so, in the procedure to calculate equvalent shrinkage strain ε^*_{sh}, the values of creep can be ignored.

In the first step of eliminating the effect of shrinkage, using the experimental moment-curvature diagram, the tension-stiffening relationship was derived using the inverse technique. The value of tension-stiffening stress σ_{ts} of HVFA-SCC is concluded to be better than that of normal concrete (NC). This means that HVFA-SCC is more stiff in resisting stresses during loading.

In the second step, using the tension-stiffening relationship obtained in the first step, the moment-curvature diagram was calculated using the direct technique. In this step, it was found that from the beginning of loading until the first crack, the curve shows a linear relationship between moment and curvature. After the first crack is reached, there is a difference in the value of the curve. After eliminating

shrinkage, a reduction in the curvature value occurs and it can be seen that the smaller the tensile reinforcement ratio, the greater the reduction in the curvature value. The curvature reduction value in HVFA-SCC is smaller than in normal concrete (NC). The overall reduction was -3.76%.

In the third step in eliminating shrinkage, the tension-stiffening relationship free of shrinkage is calculated with the inverse technique using the free of shrinkage moment-curvature diagram obtained from the second step. Shrinkage reduces the maximum tension-stiffening stress ($\sigma_{ts,max}$) by at least 1.43% and the ultimate tension-stiffening stress ($\sigma_{ts,u}$) by 72.51%. In conclusion, the calculation of tension-stiffening by eliminating shrinkage is very necessary to get more detailed and accurate calculation results.

APPENDIX A- Shrinkage and Creep Calculation

Example Shrinkage and Creep Calculation for HVFA-SCC

Typical calculation to eliminate the effects of shrinkage and creep HVFA-SCC – 12 with b = 0.15 m; h = 0.25 m; d = 0.23m; A_s = 0.0021 m^2; E_c = 27623 MPa; n = 7.24; I_{uncr} = 0.000195 m^4; I_{eff} = 0.000061 m^4; I_{cr} = 0.000056 m^4; fr = 4.028; and ε^*_{sh} = -0.0001302 MPa.

From Eq. 5 and Eq. 7, shrinkage strain,ε_{sh} of HVFA-SCC concrete with f_{cm} = 33.12MPa can be calculated as follows:

$$\beta_{RH} = -1.55\left[1-\left(\frac{0.7}{1}\right)^3\right] = -1.01835$$

An example of the calculation of the creep of HVFA-SCC concrete with f_{cm} = 33.12 MPa is as follows:

$$\beta_{(f_{cm})} = \frac{16.8}{\sqrt{f_{cm}}} = \frac{16.8}{\sqrt{33.12}} = 2.919$$

$$\beta_{(t_0)} = \frac{1}{(0{,}1 + t_0^{0,20})} = \frac{1}{(0.1 + 28^{0,20})} = 0.488$$

$$\phi_{RH} = 1 + \frac{1\text{-}70/100}{0.1.\sqrt[3]{0.250}} = 2.889$$

$$\phi_0 = (2.889)(2.919)(0.488) = 4.115$$

$$\beta_H = 1.5[1 + (0.012.70)^{18}]0.3582 + 250 = 250.391$$

The value of the coefficient of creep from Eq.8:

$$\phi(t, t_0) = (4.115)(0.502) = 2.068$$

a coefficient that shows the development of creep with time after being given loading from Eq. 9.

$$\beta_{c(t,t_0)} = \left[\frac{(28\text{-}0)}{(250.391 + (28\text{-}0))}\right]^{0,3} = 0.502$$

$$\varepsilon_{sh,HVFA} = \left[(160 + 10.4)\left(9\text{-}\frac{33.12}{10}\right)\right] x10^{-6} x(-1.01835) x\left[\frac{\frac{(28\text{-}0)}{1}}{350x\left(\frac{250}{100}\right)^2 + \frac{(28\text{-}0)}{1}}\right]^{0.5} = -0.000130 \text{ MPa}$$

Based on Kristiawan & Nugroho (2017), HVFA-SCC creep coefficient $\phi(t, t_0)$ needs to be multiplied by the ratio = (2.068)(1.39) = 2.875.

Thus, the value of the coefficient of creep from HVFA-SCC is 2.875.

Subsequently, to find the equivalent shrinkage strain value that takes into account the creep effect, ε_{sh}^{*} HVFA-SCC:

$$p = \frac{0.000212}{2(2(0{,}25)) + 2(0.15) + (0.25)0.15} = 0.000126$$

$$n = \frac{E_s}{E_C} = \frac{200000}{4800\sqrt{33.12}} = 7.667$$

$$n_t = \frac{200000}{27626.87} = 7.239$$

deformation modulus of concrete from Eq. 15:

$$E_{c,t} = \frac{4800\sqrt{33.12}}{1 + 2.875} = 27626.87 \text{ MPa}$$

The equivalent shrinkage strain value that takes into account the creep effect for HVFA-SCC from Eq. 11. The results of the calculation of equvalent shrinkage strain $\varepsilon_{sh}^{*}$of HVFA-SCC and NC concrete can be seen in Table 5.

$$\varepsilon_{sh}^{*} = -0.000130\left[\frac{1+(7.667(0.000126))}{1+(7.239(0.000126))}\right] = -0.000130 \text{ MPa.}$$

APPENDIX B- Eliminating the Effects of Shrinkage and Creep

Example to Calculate Step 1:

(HVFA SCC-12 at loading 65 kN)

From Eq. 18 - Eq. 22, we obtain $C_3 = -8.23$; $C_2 = 5.56$; $C_1 = 0.03$; $C_0 = -0.02$ and $\bar{C} = 6.30$.

The tension-stiffening stress, σ_{ts} can be calculated from Eq.16. The center of gravity of the reinforced-concrete beam cross-section can be calculated from Eq. 17.

$$a = -\frac{1}{3(-8.23)}\left\{2(6.3)\sin\left[\frac{1}{3}\arcsin\left(-\frac{(27)(-8.23^2)(-0.02)-9(-8.23)(5.56)(0.03)+2(5.56^3)}{2(6.30^3)}\right)\right]+5.56\right\} = 0.0601 \text{ m}$$

$$\sigma_{ts} = \frac{(1.16)10^{-2}}{0.00021}\left[\frac{(4800\sqrt{33.12})(0.0601^2)0.15}{2} + \left(200000-4800\sqrt{33.12}\right)(0.0601-0.029)(9{,}308)10^{-5}-200000(0.2308-0.0601)0.0002\right] = 41.29 \text{ MPa}$$

$$\varepsilon_c = (1.16)(10^{-2})(0.231-0.0601) = 0.00198; E_{ts} = 41.29/0.00198 = 20805.03 \text{ MPa};$$

Example to Calculate Step 2:

The moment-curvature diagram is calculated using the direct technique. From Eqs. 29-31, we obtain $C_2 = 2071.79$; $C_1 = 62.77$; $C_0 = -11.24$.

The distances from the top fiber of the cross-section to the center of the net concrete cross-section and the cross-sectional center of gravity of the reinforced-concrete beam can be calculated from Eq. 27 and Eq. 28 with obtained values (a=0.06 m and ac = 0.033 m). A fictitious axial force can be calculated with Eq. 25 with obtained value (Nsh = 0.0327 kN).

Bending moment and curvature-free shrinkage can be calculated from Eq. 26 and Eq. 32:

$M_{sh} = -0.00086$ KN-m;

$\varphi = \frac{0.0195+(-0.00086)}{1.677} = 0.01$.

Example to Calculate Step 3:

Using the same inverse technique as in step 1, the coefficients obtained are:

$C_3 = -7.73$; $C_2 = 5.35$; $C_1 = 0.036$; $C_0 = -0.02$ and $\bar{C} = 6.18$, *a = 0.061 m. The* tension-*stiffening stress, σ_{ts} and ε_c can be calculated:*

$$\sigma_{ts} = \frac{0.011}{0.00021}\left[\frac{4800\sqrt{33.12}(0{,}061^2)0.15}{2} + \left(200000-4800\sqrt{33.12}\right)(0.061-0.029)(9.308)10^{-5}-200000(0.231-0.061)0.00021\right]$$

$$= 59.608 \text{ MPa}$$

$\varepsilon_c = 0.011(0.2308-0.061) = 0.0018$.

REFERENCES

ACI Committee 408. (2003). “ACI 408R-03 bond and development of straight reinforcing bars in tension”. American Concrete Institute, 1-49.

ACI Committee 435. (2003). "Control of deflection in concrete structures reported by ACI committee". 435.

Alghazali, H.H., and Myers, J.J. (2019). “Bond performance of high-volume fly-ash self-consolidating concrete in full-scale beams”. ACI Structural Journal, 1, 161-170. doi: 10.14359/51706920.

Álvaro, L. et al. (2016). “Acta scientiarum tension stiffening of steel-fiber-reinforced concrete”. doi:10.4025/actascitechnol.v38i4.28077.

ASTM C39. (2005). “Standard test method for compressive strength of cylindrical concrete specimens”. ASTM International, 1-7. doi: 10.1520/C0039.

Bischoff, P.H., and Paixao, R. (2004). “Tension stiffening and cracking of concrete reinforced with glass fiber-reinforced polymer (GFRP) bars”. Canadian Journal of Civil Engineering, 31 (4), 579-588. doi: https://doi.org/10.1139/l04-025.

Castel, A., Gilbert, R.I., and Ranzi, G. (2014). “Instantaneous stiffness of cracked reinforced concrete including steel-concrete interface damage and long-term effects”. Journal of Structural Engineering, 140 (6), 04014021. doi: 10.1061/(ASCE)ST.1943-541X.0000954.

CEB-FIP Model Code. (1990). "CEB-FIP model code 1990". Edited by Thomas Telford. Switzerland.

EFNARC. (2002). "Specification and guidelines for self-compacting concrete". Edited by E. S.-G. Brian Poulson. Available at: https://static1.squarespace.com/static/5e6b93d41858c8369bc361b9/t/5f71af69b66cd43eed898fd3/1601285996901/SCC+Guidelines+02.pdf.

Elaghoury, Z. (2019). “Long-term deflections of reinforced concrete beam”. In: Proceedings of Annual Conference, Canadian Society for Civil Engineering. Electronic Thesis and Dissertation Repository. Available at: https://ir.lib.uwo.ca/etd/6496.

Gilbert, R.I. (2013). “Time-dependent stiffness of cracked reinforced and composite concrete slabs”. Procedia-Engineering, 57 (April), 19-34. doi: 10.1016/j.proeng.2013.04.006.

Gilbert, R.I., Mickleborough, N.C., and Ranzi, G. (2017). "Design of prestressed concrete to Eurocode 2". taylorfrancis.com. Available at: https://www.taylorfrancis.com/books/mono/10.1201/9781315389523/design-prestressed-concrete-eurocode-2-raymond-ian-gilbert-neil-colin-mickleborough-gianluca-ranzi.

Jalil, S., and Sultan, A.A. (2021). “Flexural strength of RC beams with partial replacement of concrete with hooked-steel fiber-reinforced concrete”. Jordan Jornal of Civil Engineering, 15 (4), 586-596. Available at: https://jjce.just.edu.jo/issues/paper.php?p=6029.pdf.

Kaklauskas, G. et al. (2011). “Tension-stiffening model attributed to tensile reinforcement for concrete flexural members”. Procedia-Engineering, 1433-1438. doi: doi:10.1016/j.proeng.2011.07.180.

Kaklauskas, G. et al. (2015). “Tension-stiffening behaviour of reinforced concrete ties of various strength classes”. Second International Conference on Performance–based and Life-cycle Structural Engineering (PLSE 2015), The University of Queensland, Brisbane, Australia, 582-590. doi: 10.14264/uql.2016.1174.

Kaklauskas, G., and Gribniak, V. (2016). “Hybrid tension stiffening approach for decoupling shrinkage effect in cracked reinforced-concrete members”. Journal of Engineering Mechanics, 142 (11), 04016085. doi: 10.1061/(asce)em.1943-7889.0001148.

Kristiawan, S.A., and Nugroho, A.P. (2017). “Creep behaviour of self-compacting concrete incorporating high-volume fly ash and its effect on the long-term deflection of reinforced-concrete beams". Procedia-Engineering, 171, 715-724. doi: 10.1016/j.proeng.2017.01.416.

Kumar, V.S., Indira, P.V., and Ganesan, N. (2019). “Tension stiffening and cracking behaviour of hybrid fibre-reinforced ternary blend geopolymer concrete”. Journal of Structural Engineering, 46, 257-266.

Pandurangan, K., and Mohan, S. (2016). “Influence of fusion-bonded epoxy-coated bars on tension stiffening of self-compacting concrete”. (February), 1-24. doi: 10.9790/1684-13132027.

Sokolov, A. et al. (2010). “Tension-stiffening model based on test data of RC beams”. 10th International Conference on Modern Building Materials, Structures and Techniques, 810-814.

Stramandinoli, R.S.B., and La Rovere, H.L. (2008). “An efficient tension-stiffening model for non-linear analysis of reinforced-concrete members”. Engineering Structures, 30 (7), 2069-2080. doi: 10.1016/j.engstruct.2007.12.022.

Tucker, B.T. (2012). “Investigation of the effects of shrinkage, creep and abrasion on self-consolidating concrete and high-volume fly ash-concrete in transportation-related infrastructure”. Master Thesis, 6899. Available at: https://scholarsmine.mst.edu/masters_theses/6899